AGU PUBLICATIONS

Geophysical Research Letters

RESEARCH LETTER
10.1002/2013GL058922

**Key Points:**
- A satellite method for estimating convective vertical velocity
- Relation between convective dynamics and internal vertical structure
- Implications for future missions design

**Correspondence to:**
Z. J. Luo,
luo@sci.ccny.cuny.edu

**Citation:**
Luo, Z. J., J. Jeyaratnam, S. Iwasaki, H. Takahashi, and R. Anderson (2014), Convective vertical velocity and cloud internal vertical structure: An A-Train perspective, *Geophys. Res. Lett.*, *41*, doi:10.1002/2013GL058922.

Received 2 DEC 2013
Accepted 7 JAN 2014
Accepted article online 8 JAN 2014

# Convective vertical velocity and cloud internal vertical structure: An A-Train perspective

**Zhengzhao Johnny Luo[1], Jeyavinoth Jeyaratnam[1], Suginori Iwasaki[2], Hanii Takahashi[3,4], and Ricardo Anderson[1]**

[1]Department of Earth and Atmospheric Sciences and NOAA-CREST Institute, City College of New York, CUNY, New York, New York, USA, [2]Department of Earth and Ocean Sciences, National Defense Academy, Yokosuka, Kanagawa, Japan, [3]Program in Earth and Environmental Sciences, the Graduate Center, CUNY, New York, New York, USA, [4]Now at Jet Propulsion Laboratory, California Institute of Technology, Pasadena, California, USA

**Abstract** This paper describes a novel use of A-Train observations to estimate vertical velocities for actively growing convective plumes and to relate them to cloud internal vertical structure. Convective vertical velocity is derived from time-delayed (1–2 min) IR measurements from MODIS and IIR. Convective vertical velocities are found to be clustered around 2–4 m/s but the distributions are positively skewed with long tails extending to larger values. Land convection during the 13:30 overpasses has higher vertical velocities than those during the 1:30 overpasses; oceanic convection shows the opposite, albeit smaller, contrast. Our results also show that convection with larger vertical velocity tends to transport larger precipitation-size particle and/or greater amount of water substance to higher altitude and produces heavier rainfall. Finally, we discuss the implications of this study for the designs of future space-borne missions that focus on fast-evolving processes such as those related to clouds and precipitation.

## 1. Introduction

Vertical velocity is a fundamental parameter for understanding convection. Much of the land-ocean contrasts in convective cloud microphysics, dynamics, and electrification can be attributed to the differences in vertical velocities [*Lucas et al*., 1994; *Williams et al*., 2002]. In global climate model, convective vertical velocity and the associated convective mass flux play a controlling role in determining the collective effects of cumulus ensemble on the large-scale environment [*Arakawa and Schubert*, 1974]. Traditional cumulus schemes hide convective vertical velocity in bulk convective mass flux term, but recent developments and applications seek to treat it explicitly so that subgrid-scale processes associated with convection can be better represented and diagnosed [e.g., *Donner et al*., 2001; *Gregory*, 2001; *Del Genio et al*., 2007].

Unlike many other aspects of convective clouds, vertical velocity is extremely difficult to observe. The most direct measurements come from instrumented aircraft that penetrate convective clouds [e.g., *LeMone and Zipser*, 1980a, 1980b; *Lucas et al*., 1994]. However, such measurements are rare due to safety concerns. Another source of information on convective vertical velocity comes from ground-based or airborne Doppler radars [e.g., *Heymsfield et al*., 2010]. In this study, we draw on satellite observations. An obvious advantage of using satellite data is global coverage, which enables us to generalize our findings. Since no space-borne Doppler radar is available at this time, alternative method needs to be developed.

*Adler and Fenn* [1979] used change rate of cloud top temperature (CTT) with time to estimate vertical velocity (w) of convective tops, which can be expressed as: $w = \frac{dT_B/dt}{\partial T/\partial z}$ (equation (1)), where $T_B$ is IR brightness temperature which is used to represent CTT, and $\partial T/\partial z$ is the moist adiabatic lapse rate. In their study, time evolution of CTT was derived from rapid scan of geostationary (GEO) satellite data. The requirement to observe time evolution makes it difficult to apply the technique to a polar-orbiting or low earth orbiting (LEO) satellite because a LEO satellite can hardly see the same convective element a second time. However, the formation fly of the A-Train constellation offers a rare opportunity to exploit the small time difference (1–2 min) between MODIS (Moderate Resolution Imaging Spectroradiometer) onboard Aqua and IIR (Imaging Infrared Radiometer) onboard CALIPSO (Cloud-Aerosol Lidar and Infrared Pathfinder Observation) for studying vertical velocity. Both MODIS and IIR have IR window channel near 11 μm with similar spatial resolution (1 km). $\partial T/\partial z$ is assumed to be the moist adiabatic lapse, which is mostly a function of temperature. For the cases analyzed in this study, it ranges from around 5.5 K/km

when temperature is high (or cloud top is low) to nearly dry adiabatic lapse rate at about 9.8 K/km when temperature is low (or cloud top is high).

Compared to GEO satellites, there are several benefits associated with using the A-Train data for studying detailed convective processes. First, the spatial resolution of MODIS and IIR in the thermal IR is 1 km, whereas that of the current GEO is only 4 km. In situ observations showed that the size of typical active convective updrafts is about 1 km or less [*Braham*, 1952; *LeMone and Zipser*, 1980a]. Four-kilometer resolution will smear out the detail associated with convective elements. Likewise, the small temporal separation between IIR and MODIS (1–2 min) makes it valuable for capturing the quick evolution of small-scale structures related to intense convective turrets. Second, MODIS and IIR are part of the A-Train constellation with a host of advanced cloud measurements that will greatly enhance the scientific value of the estimated convective vertical velocities. For example, CloudSat and CALIPSO carry active sensors—cloud-profiling radar (CPR) and Cloud-Aerosol Lidar with Orthogonal Polarization (CALIOP)—that offer glimpses of the internal vertical structures of the convective clouds. They allow for correlative study of convective dynamics and cloud microphysics.

The objective of this article is to describe the method we used to estimate convection vertical velocity (section 2) and present some initial results (section 3). This is the first of a series of papers we are developing along the line of exploiting time difference among A-Train members for studying convective dynamics. Here, we focus on investigating the connection between convective vertical velocity and cloud internal vertical structure. Section 4 summarizes this work and discusses follow-on studies and implications for future mission designs.

## 2. Data and Methodology

### 2.1. Data From the A-Train Constellation

The A-Train constellation consists of a suite of satellites that fly in close formation in a sun-synchronous orbit with the local equator crossing time at ~ 1:30 am/pm [*Stephens et al*., 2002; *L'Ecuyer and Jiang*, 2010]. Here, we briefly describe the three instruments and satellites that are used in this study and the relevant measurements: MODIS (on board Aqua), IIR (on board CALIPSO), and CPR (on board CloudSat).

MODIS is an optical imaging radiometer with 36 channels from 0.4 μm to 14.2 μm at varying spatial resolution from 250 m to 1 km. In this study, we use channel 31, which is located at the IR window region (11.03 μm) and provides a means to estimate CTT. IIR is a three-channel imaging radiometer on board CALIPSO [*Winkers et al*., 2009] that is intended to provide the context of the lidar measurements. It has a similar IR window channel centering at 10.6 μm (calibration between the two measurements will be described in section 2.3). Both MODIS and IIR IR window channels have similar spatial resolution of 1 km. Aqua flies ahead of CALIPSO by 1–2 min so MODIS sees a cloud a little earlier than IIR.

CPR is a millimeter-wavelength radar on board CloudSat that is sensitive to both cloud- and precipitation-size particles [*Stephens et al*., 2008]. Its footprint is approximately 1.7 km along track and 1.3 km across track, and the vertical resolution is 480 m, oversampled to 240 m. The radar reflectivity profiles from CPR provide information on cloud microphysics and internal vertical structure. CloudSat and CALIPSO are closely synchronized with each other with CloudSat being ahead of CALIPSO by only 10–15 s.

### 2.2. Selection of Convective Updrafts

Active convective updrafts usually appear in the IR brightness temperature ($BT_{IR}$) image as local minima [e.g., *Bedka et al*., 2012]. So, we start our selection procedure by identifying such local minima pairs in IIR and MODIS $BT_{IR}$ measurements. Due to small cloud movement and parallax shift [*Wang et al*., 2011], the minimum $BT_{IR}$ from MODIS could be registered a few km away from that from IIR. To accommodate for these displacements, we allow for a 5 km window in search of the minimum $BT_{IR}$ pairs from the two measurements. Only the cases where IIR $BT_{IR}$ is lower than that of MODIS by more than 1 K are retained, which represent actively growing convective updrafts. The 1 K buffer is intended to account for the calibration uncertainty between IIR and MODIS (see detail in section 2.3).

Since CloudSat is an important component of this study that provides information on cloud microphysics and convective internal structure, we only keep the selected IIR/MODIS $BT_{IR}$ pairs that are within 5 km of the CloudSat observations. We further require that CloudSat CPR profiles show characteristics of convective cores, which, based on our recent studies [e.g., *Luo et al*., 2010; *Takahashi and Luo*, 2012], are defined as

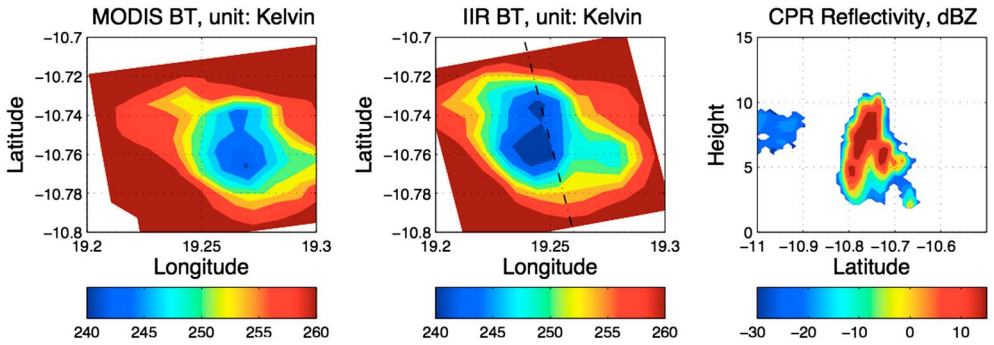


**Figure 1.** Brightness temperature (unit: Kelvin) from (left) IIR and (middle) MODIS. The dashed line shows the CALIPSO/CloudSat footprint. (Right) CloudSat reflectivity profile (unit: dBZ) along the dashed line.

profiles meeting the following criteria: (1) continuous radar echo from cloud top to within 2 km of the surface, (2) cloud top height (CTH) $\geq$ 6 km (this condition eliminates shallow convective clouds because they tend to be small and are not well captured by CloudSat), (3) the maximum radar echo is greater than 10 dBZ and occurs above 6 km, and the vertical separation between CTH and 10 dBZ echo top height (ETH) is within 2 km. The third condition effectively eliminates the stratiform part of a convective system and retains only the convective cores. Figure 1 shows an example of a growing convective element that was selected by this procedure. Two years of data (2008–2009) were analyzed. We focus on the tropical region (30°S–30°N) in this study. A total of 940 convective updraft elements were selected.

### 2.3. Intercalibration Between MODIS and IIR $BT_{IR}$

Since the two $BT_{IR}$ measurements are made from different instruments on board different platforms, it is important to intercalibrate them. This is a relative calibration problem because only the $BT_{IR}$ difference enters equation (1). To avoid the parallax shift between MODIS and CALIPSO [*Wang et al.*, 2011], we use clear pixels (as indicated by collocated CloudSat data) as our calibration targets. Collocated IIR and MODIS clear pixels from the whole globe are used to compute $\Delta BT_{IR} \equiv BT_{IR}(IIR) - BT_{IR}(MODIS)$ as a function of $BT_{IR}$. Results show that $\Delta BT_{IR}$ is relatively small (~ 0.5 K) when $BT_{IR}$ is warm ($>$ 260 K) but starts to increases as $BT_{IR}$ decreases. At the cold end of clear cases ($BT_{IR}$ ~ 225 K), $\Delta BT_{IR}$ increases to 1.4 K. For $BT_{IR} < 225$ K, $\Delta BT_{IR}$ are extrapolated from the clear observations. We also tried to use high-level clouds for calibrating $BT_{IR} < 225$ K; results are noisy due to parallax shift but the mean differences are similar to the extrapolation results. The standard deviation of $\Delta BT_{IR}$ is about 1 K, which represents our uncertainty.

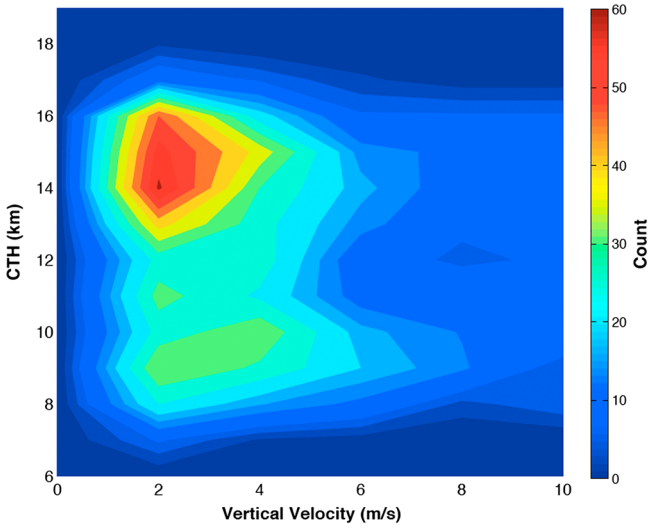


**Figure 2.** Histogram of convective vertical velocity as a function of cloud top height (CTH) for actively growing convective plumes in the tropics (30°S–30°N).

## 3. Results

Figure 2 shows the histogram of the estimated convective vertical velocity as a function of CTH. We first note that tropical convection selected in this study fall into two modes: one has CTH near 8–10 km and the other has CTH around 14–15 km. They correspond to cumulus congestus and deep convection, respectively, as described in *Johnson et al.* [1999]. CTHs of the cumulus congestus are significantly higher than the melting level (~5 km in the tropics), which is suggested by *Johnson et al.* [1999] as a weak stable layer inhibiting convective development. Likewise, CTHs of the selected deep

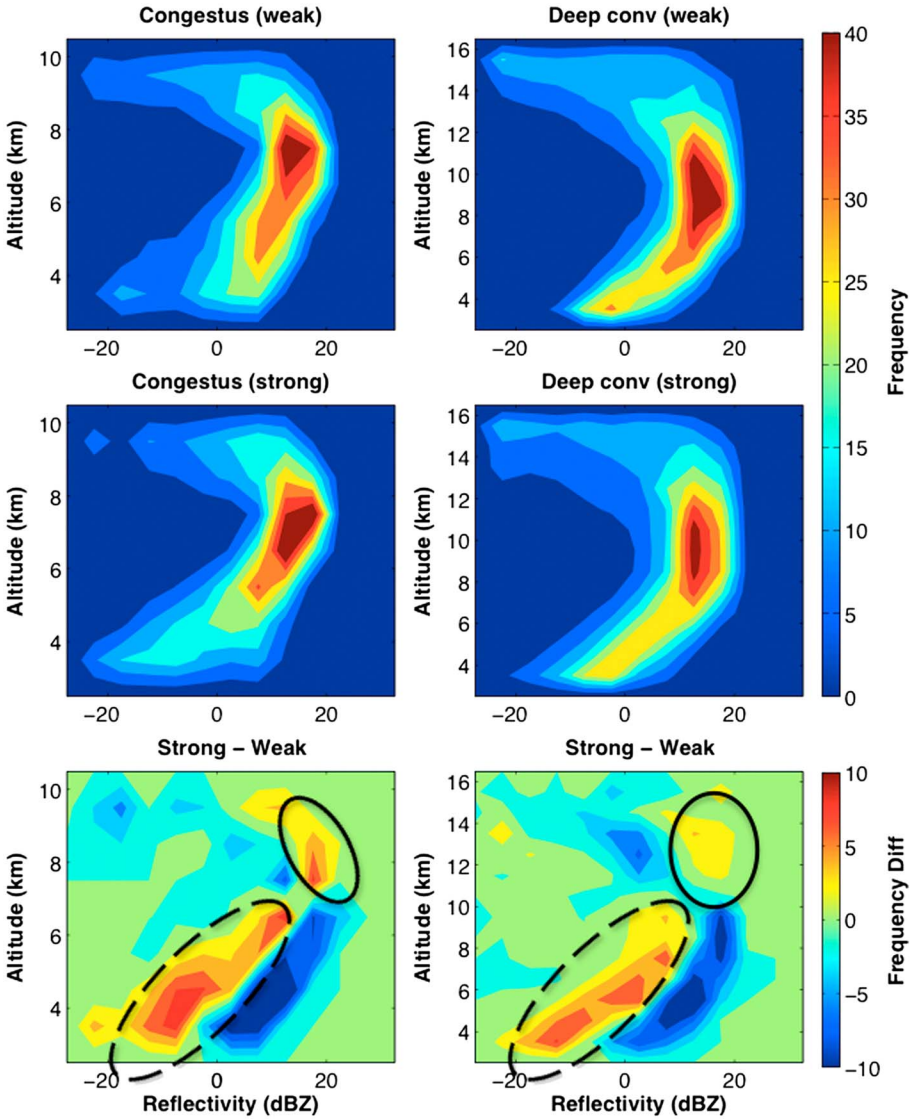


**Figure 3.** Contoured frequency by altitude diagram (CFAD) for CloudSat CPR reflectivities. The left and right panels are for cumulus congestus and deep convection, respectively. Weak (first row) and strong (second row) convective plumes are treated separately, along with the differences between them (third row).

convection are also somewhat higher than the level of neutral buoyancy for tropical deep convective regions, which is estimated to be ~13.4 km [*Takahashi and Luo*, 2012]. These higher CTHs are most likely due to overshooting because our selection criteria (section 2.2) favor actively developing convective plumes.

The cumulus congestus mode is worth some additional discussion. *Luo et al*. [2009] classified the snapshot observations of apparent cumulus congestus into those that cease growth at the intermediate level (*terminal* cumulus congestus) and those that will continue to ascend (*transient* cumulus congestus) by comparing cloud top temperature with the ambient temperature of the same height level. *Luo et al*. [2010] and *Wang et al*. [2011] further analyzed cloud top buoyancy and found that *transient* cumulus congestus (i.e., convective plumes with positive buoyancy) account for ~ 70% of the convective cores with CTH near 6–10 km. Obviously, the cumulus congestus mode identified here corresponds to the *transient* cumulus congestus; some of them may later develop into deep convection.

Figure 2 shows that convective vertical velocities are clustered around 2–4 m/s. Roughly, 2 m/s corresponds to our cutoff in $\Delta BT_{IR}$ at 1 K; smaller $\Delta BT_{IR}$ (and vertical velocities) are difficult to be distinguished from noises. Despite this limitation, the vertical velocity distributions show positive skewness with long tails extending to higher velocity

values significantly above our detection limit. It is reasonable to speculate that fast-growing convective plumes possess different cloud microphysical and dynamical character than those that grow slowly. The A-Train constellation provides an opportunity to explore such question from a space-borne perspective. As a first step, we analyze collocated CloudSat radar reflectivity profiles to illustrate how convective dynamics is connected to cloud microphysics and internal vertical structures. Specifically, we compare the characteristics of CPR reflectivity profiles between strong and weak convection, as indicated by convective vertical velocities.

Radar reflectivity profiles can be conveniently summarized in contoured frequency by altitude diagram (CFAD) originally proposed by *Yuter and Houze* [1995]. Figure 3 shows the CFADs for strong and weak convection, defined as convective plumes whose vertical velocities belong to the largest one third and the smallest one third of the distributions, respectively (which correspond to $w < 2.7$ m/s and $> 4.8$ m/s, respectively, for cumulus congestus and $w < 2.4$ m/s and $> 4.2$ m/s, respectively, for deep convection). The left columns are for cumulus congestus (CTH between 8 and 10 km) and the right columns for deep convection (CTH between 13 and 16 km). The contoured frequencies are normalized at each level (so they add up to 100 at each level). The bow shape of these CFADs is typical of convective cores observed by millimeter-wavelength radar from space: the bulging part with reflectivity of ~20 dBZ near cloud top reflects signals from large precipitation-size particles before attenuation starts to affect the reflectivity, while the tail near the surface with very small reflectivity is due to severe attenuation of radar signals by heavy rains above.

The most intriguing feature in Figure 3 lies in the difference between the CFADs of strong and weak convection (the third rows). For both cumulus congestus and deep convection, stronger convective plumes show more occurrences of large radar echo (~15–20 dBZ) near cloud top, which we highlight with dark solid ovals. This suggests that more intense convection is better capable of transporting larger particles and/or greater amount of water substance to higher altitude, although it is possible that larger amount of condensate brings about more latent heat release that may further fuel convective updraft. Meanwhile, the more intense convective plumes also show more severe attenuation in radar signals at the lower levels, as highlighted by dark dashed ovals. This suggests that stronger convection produces heavier rainfall.

Land-ocean and day-night (13:30 versus 1:30 overpasses) contrasts are investigated. A couple of results are worth noting: (1) For the afternoon (13:30) convection, 37% of the selected cases occur over land (but keep in mind land only occupies 26% of the tropics). For the early morning (1:30) convection, only 14% occur over land; majority of them are found over ocean. This is consistent with previous finding concerning the diurnal cycles of oceanic and continental convection [e.g., *Liu and Zipser*, 2008]. (2) Over land, the mean vertical velocities for afternoon and early morning convection are, respectively, 5.1 m/s and 4.1 m/s, suggesting that convection is more vigorous in the afternoon than in the early morning, although we acknowledge that A-Train misses the peak stage of continental convection, which is in the late afternoon. Over ocean, the mean vertical velocities for afternoon and early morning are, respectively, 4.5 m/s and 5.0 m/s.

Finally, we briefly compare our study with previous work and discuss sources of error. *Adler and Fenn* [1979] used a similar method to estimate convective vertical velocity, although the spatial resolution of their IR data is only 8–10 km. They manually identified some strong convection in Oklahoma during the tornado season. Except for severe tornadic elements, the mean values from their study are about 2–3 m/s, which are generally smaller than our estimates in this study. The main reason for the difference is probably spatial resolution because the size of active convective updrafts is about 1 km or less [e.g., *LeMone and Zipser*, 1980a].

The errors for the estimated vertical velocity come from the following sources, as also discussed in *Adler and Fenn* [1979]: (1) Use of moist adiabatic lapse rate ($\gamma_m$) to relate cloud-top cooling rates to cloud-top vertical velocity. Mixing with the ambient air may make the cooling rate differ from $\gamma_m$, although the level of the mixing is minimal during the actively growing stage of convective development [*Luo et al.*, 2008]. (2) Cloud emissivity difference between IIR and MODIS. MODIS views convection from a slantwise angle up to 17 degrees [*Wang et al.*, 2011], while IIR makes nadir observations (due to our requirement that CloudSat and CALIPSO pass through the convection). The difference in IR emission levels is approximately $H[1-\cos(17^0)] \approx 0.04H$, where H is the depth of the IR emission level. Our calculation using a radiative transfer model shows that for convective cores, H is smaller than 0.7 km, which leads to a merely 28 m difference in the IR emission levels between IIR and MODIS, or ~0.28 K in temperature difference. So, we consider this error small for our application. Ground-based measurements will provide ultimate validation of our method. Recent surface observations using continuous stereo photogrammetry of convective clouds provide a direct measure of the convective top growth rate (D. Romps, personal communication, 2013). Our future study will pursue this validation.

## 4. Summary and Discussions

This short letter describes a novel application of the A-Train data that allows for estimation of convective vertical velocity and correlative analysis of convective dynamics, cloud microphysics, and cloud internal vertical structures. Convective vertical velocity is derived from time-delayed (1–2 min) IR brightness temperature measurements from MODIS and IIR. The method is similar to a previous study using rapid scans of GEO data, but several benefits come with the use of A-Train data such as higher spatial resolution that is more in line with the size of convective updrafts and added scientific value of the estimated convective vertical velocity owing to synergistic measurements of other cloud parameters.

Principal findings of the study are as follows: (1) Two convective modes are identified for actively growing convective plumes, which correspond, respectively, to cumulus congestus and deep convection. But some of the congestus may grow into deep convection at a later time — a type that is called *transient* cumulus congestus by *Luo et al*. [2009]. (2) The histogram of convective vertical velocity shows clusters around 2–4 m/s, but the distribution is positively skewed with long tails extending to higher velocity values. Land convection during the 13:30 overpasses has higher vertical velocities than those during the 1:30 overpasses; oceanic convection shows the opposite, albeit small contrast between the afternoon and early morning overpasses. (3) Subsetting CloudSat CPR reflectivity profiles by convective vertical velocity shows that stronger convection is capable of transporting larger precipitation-size particle and/or greater amount of water substance to higher altitude and tends to produce heavier rainfall.

Some of these results concerning convective climatology and relation between convective dynamics, microphysics, and internal vertical structures may be expected from our general understanding of tropical convection, at least qualitatively. Nevertheless, it is important to point out that our current study demonstrates the capability to use synergistic space-borne measurements, together with novel analysis method, to quantitatively explore these questions from a global perspective. The same analysis framework can be expanded to other correlative measurements from both the A-Train and other satellites. Such studies will bring new insights and provide important observational constraints for evaluating GCM cumulus parameterizations.

This article is the first of a series of studies we are developing along the line of exploiting time difference among different A-Train members for studying convective dynamics. Two key elements underline this type of study: (1) well-paced time separation between instruments making similar measurements that can be used to derive time evolution of certain convective cloud parameters and (2) correlative data sets that provide simultaneous and complementary measurements of other aspects of clouds. MODIS and IIR fulfill the first requirement. CloudSat, on the other hand, brings in simultaneous snapshot observations of cloud microphysics and internal vertical structure. To this end, other A-Train measurements such as CALIPSO, AMSR-E, and visible/near-IR channels of MODIS can all add additional information that will give a more complete depiction of the convective clouds.

The two key elements discussed above have implications for the designs of future cloud missions or more generally, any mission that focuses on fasting-evolving phenomena or processes on the order of minutes or several tens of minutes. First, it is constructive to consider deploying inexpensive sensors in a time-delayed constellation so that certain processes can be captured in time evolution. Capturing time evolution can also be achieved by using GEO satellites, but LEO provides higher spatial resolution (thus good for small-scale processes) and offers other technological advantages. Second, this time-delayed constellation may be supplemented by other members that provide certain advanced snapshot measurements.

**Acknowledgments**

We would like to thank William Rossow, Hajime Okamoto, Hiro Masunaga, and B. J. Sohn for helpful comments and insightful discussions. The study was supported by two NASA grants awarded to CUNY: NNX10AM31G and NNX12AC13G. We also thank Graeme Stephens and Ziad Haddad for supporting this work and follow-on analysis. SI was supported by the Japan Society for the Promotion of Science, Grant-in-Aid for Young Scientists (B) 24710024.

The Editor thanks two anonymous reviewers for assistance evaluating this manuscript.

## References

Adler, R. F., and D. D. Fenn (1979), Thunderstorm vertical velocities estimated from satellite data, *J. Atmos. Sci.*, *36*, 1747–1754.

Arakawa, A., and W. H. Schubert (1974), Interaction of cumulus cloud ensemble with the large-scale environment, Part I, *J. Atmos. Sci.*, *31*, 674–701.

Bedka, K. M., R. Dworak, J. Brunner, and W. Feltz (2012), Validation of satellite-based objective overshooting cloud-top detection methods using CloudSat cloud profiling radar observations, *J. Appl. Meteorol. Climatol.*, *51*, 1811–1822.

Braham, R. R., Jr. (1952), The water and energy budgets of the thunderstorm and their relation to thunderstorm development, *J. Meteorol.*, *9*, 227–242.

Del Genio, A. D., M.-S. Yao, and J. Jonas (2007), Will moist convection be stronger in a warmer climate?, *Geophys. Res. Lett.*, *34*, L16703, doi:10.1029/2007GL030525.

Donner, L. J., C. J. Seman, and R. S. Hemler (2001), A cumulus parameterization including mass fluxes, convective vertical velocities, and mesoscale effects: Thermodynamic and hydrological aspects in a general circulation model, *J. Clim.*, *14*, 3444–3463.

Gregory, D. (2001), Estimation of entrainment rate in simple models of convective clouds, *Q. J. R. Meteorol. Soc.*, *127*, 53–72.

Heymsfield, G. M., L. Tian, A. J. Heymsfield, L. Li, and S. Guimond (2010), Characteristics of deep tropical and subtropical convection from nadir-viewing high-altitude airborne Doppler radar, *J. Atmos. Sci.*, *67*, 285–308.

Johnson, R. H., T. M. Rickenbach, S. A. Rutledge, P. E. Ciesielski, and W. H. Schubert (1999), Trimodal characteristics of tropical convection, *J. Clim.*, *12*, 2397–2418.

L'Ecuyer, T., and J. H. Jiang (2010), Touring the atmosphere aboard the A-Train, *Phys. Today*, *63*(7), 36–41.

LeMone, M. A., and E. J. Zipser (1980a), Cumulonimbus vertical velocity events in GATE. Part I: Diameter, intensity and mass flux, *J. Atmos. Sci.*, *37*, 2444–2457.

LeMone, M. A., and E. J. Zipser (1980b), Cumulonimbus vertical velocity events in GATE. Part II: Synthesis and model core structure, *J. Atmos. Sci.*, *37*, 2458–2469.

Liu, C., and E. J. Zipser (2008), Diurnal cycles of precipitation, clouds, and lightning in the tropics from 9 years of TRMM observations, *Geophys. Res. Lett.*, *35*, L04819, doi:10.1029/2007GL032437.

Lucas, C., E. Zipser, and M. A. LeMone (1994), Vertical velocity in oceanic convection off tropical Australia, *J. Atmos. Sci.*, *51*, 3183–3193.

Luo, Z., G. Y. Liu, and G. L. Stephens (2008), CloudSat adding new insight into tropical penetrating convection, *Geophys. Res. Lett.*, *35*, L19819, doi:10.1029/2008GL035330.

Luo, Z., G. Y. Liu, G. L. Stephens, and R. H. Johnson (2009), Terminal versus transient cumulus congestus: A CloudSat perspective, *Geophys. Res. Lett.*, *36*, L05808, doi:10.1029/2008GL036927.

Luo, Z. J., G. Y. Liu, and G. L. Stephens (2010), Use of A-Train data to estimate convective buoyancy and entrainment rate, *Geophys. Res. Lett.*, *37*, L09804, doi:10.1029/2010GL042904.

Stephens, G. L., et al. (2002), The CloudSat mission and the A-Train: A new dimension of space-based observations of clouds and precipitation, *Bull. Am. Meteorol. Soc.*, *83*, 1771–1790.

Stephens, G. L., et al. (2008), CloudSat mission: Performance and early science after the first year of operation, *J. Geophys. Res.*, *113*, D00A18, doi:10.1029/2008JD009982.

Takahashi, H., and Z. Luo (2012), Where is the level of neutral buoyancy for deep convection?, *Geophys. Res. Lett.*, *39*, L15809, doi:10.1029/2012GL052638.

Wang, C., Z. J. Luo, and X. L. Huang (2011), Parallax correction in collocating CloudSat and MODIS observations: Method and application to convection study, *J. Geophys. Res.*, *116*, D17201, doi:10.1029/2011JD016097.

Williams, E., et al. (2002), Contrasting convective regimes over the Amazon: Implications for cloud electrification, *J. Geophys. Res.*, *107*(D20), 8082, doi:10.1029/2001JD000380.

Winkers, D. M., M. A. Vaughan, A. Omar, Y. Hu, and K. A. Powell (2009), Overview of the CALIPSO mission and CALIOP data processing algorithms, *J. Atmos. Oceanic Technol.*, *26*, doi:10.1175/2009JTECHA1281.1.

Yuter, S. E., and R. A. Houze (1995), Three-dimensional kinematic and microphysical evolution of Florida cumulonimbus. Part II: Frequency distributions of vertical velocity, reflectivity, and differential reflectivity, *Mon. Weather Rev.*, *123*, 1941–1963.